The total noise of a laser amplifier consists of signal-spontaneous beat noise, spontaneous–spontaneous beat noise, amplified-signal shot noise and spontaneous-emission shot noise. The beat noise components are dominant, so that from Reference 10, the variance of the photon number σ^2 at the amplifier output may be given as

$$\sigma^2 = 2G(G-1)n_{sp}\chi \frac{P}{E} + (G-1)^2 m_t \,\Delta f_2\, n_{sp}^2 \qquad (1)$$

where G is the peak cavity gain, n_{sp} is the population inversion parameter, χ is the excess noise factor, P is the mean input power, E is the photon energy, m_t is the number of effective transverse modes and Δf_2 is the normalised beat noise bandwidth.

For amplifiers such as those studied, where the antireflection coating is broadband, the noise is only slightly wavelength dependent and varies with n_{sp} such that, from Reference 11

$$n_{sp} = \frac{N}{N - N_0} \cdot \frac{g(N, \omega)}{g(N, \omega) - \alpha(\omega)} \qquad (2)$$

where N is the carrier density, N_0 is the transparency density, $g(N, \omega)$ and $\alpha(\omega)$ are the material gain and loss coefficients per unit length, respectively, and ω is defined as the ratio of velocity of light to wavelength.

$$n_{sp} \propto \frac{g}{g - \alpha} = \frac{\text{contrast}}{\text{gain}} \qquad (3)$$

The ratio of contrast to gain in our measurements varies by a factor of 3, principally at short wavelengths. F (noise figure) $= 2n_{sp}$, thus F only varies by 8dB. The wavelength variation of noise is not important for semiconductor amplifier switches operated at the gain peak and longer wavelengths.

Conclusion: The switching speed and the wavelength dependence of contrast and noise in MQW and bulk PBH amplifier switches have been compared. The measurements suggest that to simultaneously minimise noise and maximise contrast, the switches should be operated at the gain peak of the amplifier. High contrast was obtained with both structures. The MQW device was found to have a contrast of 41 dB and a speed of 1·2GHz at 1·51 μm, whereas the bulk device was found to have a contrast of 58dB and a speed of 400MHz. We thus conclude that MQW devices are more suitable for use as fast switches.

B. P. CAVANAGH
I. W. MARSHALL
G. SHERLOCK
H. WICKES

British Telecommunications Research Laboratories
Martlesham Heath
Ipswich IP5 7RE, United Kingdom

26th November 1990

References

1 YAMAMOTO, H., and OGIWARA, H.: 'Moving optical fiber switch experiment', *Appl. Opt.*, 1978, **17**, pp. 3675–3678
2 VESELKA, J. J., MURPHY, T. O., HERR, D. A., WATSON, J. E., MILBRODT, M. A., BAHADONI, K., DAUTARTAS, M. F., KEMMERER, C. T., MOSER, D. T., and SCHELLING, A. W.: 'A low-voltage low-crosstalk 8 × 8 Ti : $LiNbO_3$ switch for a time multiplexed switching system'. Proc. of Optical Fibre Communication Conf., Houston, Texas, February 1989, p. 135
3 IKEDA, M.: 'Switching characteristics of a laser diode switch', *IEEE J. Quantum Electron.*, 1983, **QE-19**, (2), pp. 157–164
4 OKU, S., YOSHINO, K., and IKEDA, M.: 'Design and performance of monolithic LD optical matrix switches'. Proc. of international topical meeting on photonic switching, Kobe, Japan, April 1990, 13C-17
5 OBERG, M. G., and OLSSON, N. A.: 'Wavelength dependence of the noise figure of a travelling wave InGaAsP/InP laser amplifier', *Electron. Lett.*, 1988, **24**, pp. 99–100
6 MACE, D. A. H., ADAMS, M. J., and DEVLIN, W. J.: 'High-frequency optical bistability in semiconductor optical amplifiers'. Topical Meeting on 'Nonlinear dynamics in optical systems', 4th–8th June 1990, Oklahoma, Technical Digest, **WA6-2**, pp. 272–274
7 COOPER, D. M., SELTZER, C. P., AYLETT, M., ELTON, D. J., HARLOW, M., WICKES, H., and SPILLETT, R. E.: 'High power 1·5 μm all MOVPE buried heterostructure graded index separate confinement multiple quantum well lasers'. ECOC Proceedings 3, Session 2, PDB-10, 10th–14th September 1989
8 LEALMAN, I. F., COOPER, D. M., MCILROY, P. W. A., COCKBURN, A. J., COLE, S., HARLOW, M., and SKEATS, A. P.: 'Reliable 1·3 μm high speed trenched buried heterostructure lasers grown entirely by atmospheric MOVPE', *IEE Proc. J*, 1990, **137**, (1), pp. 2–6
9 EISENSTEIN, G.: 'Gain and gain saturation spectra in 1·5 μm multiple quantum well optical amplifiers', *Appl. Phys. Lett.*, July 1990, **57**, (4)
10 O'MAHONY, M. J.: 'Semiconductor laser optical amplifiers for use in future fiber systems', *J. Lightwave Technol.*, 1988, **6**, (4), pp. 531–544
11 MUKAI, T., YAMAMOTO, Y., and KIMURA, T.: 'S/N and error rate performance in AlGaAs semiconductor laser preamplifier and linear repeater systems', *IEEE Trans.*, 1982, **MTT-30**, (10), pp. 1548–1556

TRACKING A MANOEUVRING TARGET WITH CORRELATED MEASUREMENT NOISES BY MANOEUVRE DETECTION METHOD

Indexing terms: Radar, Noise

The tracking problem for a manoeuvring target with correlated measurement noises is considered in this letter. A modified manoeuvre detection method with the decorrelation process is employed for tracking the manoeuvring target. From computer simulation, it can be seen that the system performance can be improved significantly if the effect of noise-correlation is considered.

Introduction: The measurement noise of noisy radar data is usually assumed to be white and a conventional Kalman filter is often used for tracking nonmanoeuvring targets. If the target is manoeuvring, the conventional Kalman filter must be modified to keep the tracking performance. There have been several approaches to this problem.[1]

In practical measurement, noises are not white. Noises are autocorrelated within a bandwidth of typically a few Hertz. In many modern radar systems, the measurement frequency is usually high so that the correlation cannot be ignored. Treating the correlation noise as a first order Markov process, the noise can be decorrelated in such a way that the (modified) Kalman filter is effective after decorrelation.[2–4]

In this Letter, a modified manoeuvre detection method with the decorrelation process is employed for tracking the manoeuvring target. This method is simple and has moderate tracking performance. It has an extra advantage over other approaches[3,4] in that, even if some of the parameters about noise-correlation are unknown, these unknown parameters can be easily estimated.[5]

System model: Modelling the manoeuvre variable (acceleration) as a first order autoregressive process and treating the acceleration as part of the state vector, Singer[6] derived the target motion and radar measurement models for the manoeuvring target as

$$X_{k+1} = \phi X_k + G w_k \qquad (1)$$

$$Z_k = H X_k + v_k \qquad (2)$$

where X_k, Z_k, w_k and v_k are target state, measurement data, process noise and measurement noise, respectively. The coefficient matrices ϕ, G, H, and $Q(= E\{w_k w_k^T\})$ were shown in Reference 6.

If the measurement noise v_k is white, the system governed by eqns. 1 and 2 can be processed by the conventional Kalman filter. When the measurement frequency is high, the measurement noise is correlated. Assume that the measurement noise can be modelled as a first-order Markov process.[2]

$$v_k = \lambda v_{k-1} + v_k \quad (3)$$

where the noise coefficient $\lambda = e^{-\beta T}$, β is the noise coefficient in continuous form. The noise v_k is a zero-mean white Gaussian noise.

To decorrelate the correlated noise v_k, new measurement data $Y_k(= Z_k - \lambda Z_{k-1})$ can be generated as follows[3,4] so that the conventional Kalman filter can be applied:

$$Y_k = H^* X_k + v_k^* \quad (4)$$

where

$$H^* = H - \lambda H \phi^{-1}$$
$$B = \lambda H \phi^{-1} = (H - H^*)$$
$$v_k^* = B w_{k-1} + v_k$$
$$R^* = E\{v_k^* v_k^{*T}\} = BQB^T + (1 - \lambda^2)R \quad (5)$$

Manoeuvre detection: Tracking the manoeuvring target in this way assumes the target is always manoeuvring. When the target is in a nonmanoeuvring condition, some noises will be treated as if the target is manoeuvring. The estimation errors for both position and velocity are increased when this occurs. To enhance the performance in the nonmanoeuvring period, the manoeuvre detection method[7] is frequently used. In general, the tracking system works well in the nonmanoeuvring mode. A manoeuvre detector operates simultaneously to monitor the occurrence of a manoeuvre. When a manoeuvre is detected, the system switches to manoeuvring mode until the manoeuvre is observed to disappear. The system then reverts to nonmanoeuvring mode.

When the measurement noise is white, the innovation $\varepsilon_k(= Z_k - H\hat{X}_{k|k-1})$ is the most commonly used data in detecting a manoeuvre. Let $\sigma_k = \varepsilon_k M_k^{-1} \varepsilon_k^T$, where $M_k(= HP_{k|k-1}H^T + R)$ is the variance of ε_k. Then a fading memory scheme detection rule may be defined as follows:[7]

$$\delta_k \begin{matrix} > t_1 \\ \leq t_1 \end{matrix} \qquad \begin{matrix} \text{manoeuvring} \\ \text{nonmanoeuvring} \end{matrix} \quad (6)$$

where

$$\delta_k = \rho \delta_{k-1} + \sigma_k \quad (7)$$

The detection threshold t_1 is selected according to the probability of a tolerable false manoeuvre declaration activated by noise.

When the system works in manoeuvring mode, the acceleration is being monitored. If the acceleration is statistically insignificant, the manoeuvre is considered to disappear and the system reverts to nonmanoeuvring mode. Let $\delta_k^a = \hat{a}_k M_{k|k}^{a-1} \hat{a}_k$ where $M_{k|k}^a$ is the variance of $\hat{a}_k$ activated by the noise. Then, the following detection rule is used:[7]

$$\sum_{j=k-p_2+1}^{k} \sigma_j^a \begin{matrix} < t_2 \\ \geq t_2 \end{matrix} \qquad \begin{matrix} \text{nonmanoeuvring} \\ \text{manoeuvring} \end{matrix} \quad (8)$$

The threshold t_2 is selected according to the probability of tolerable false acceleration activated by noise.

The detection rule (eqn. 6) is good when the measurement noise is white. When the measurement noise is correlated, the noise can be decorrelated by the decorrelation process mentioned in preceding section and the innovation $\varepsilon_k^*(= Y_k - H^*\hat{X}_{k|k-1})$ is produced in the decorrelated system. It can be found that ε_k^* is not a sensitive parameter for manoeuvre detection because the data $Y_k(= Z_k - \lambda Z_{k-1})$ will lose some manoeuvring information in the subtraction process. To overcome this problem, a new innovation $\bar{\varepsilon}_k(= Z_k - H\hat{X}_{k|k-1})$ with (approximate) variance $\bar{M}_k(= HP_{k|k-1}H^T + R)$ can be generated to replace ε_k^*. In $\bar{\varepsilon}_k$, the data $\hat{X}_{k|k-1}$, $P_{k|k-1}$ are estimated in the decorrelated system, and Z_k, H and R are the measurement data and system parameters before decorrelation. This mixed structure may have good manoeuvre detection capability in the presence of correlated measurement noise. On the other hand, to detect the target reverting from manoeuvring to nonmanoeuvring state by the detection rule (eqn. 8), the decorrelated system works well.

Simulation results: A Monte Carlo simulation with 100 runs was performed to demonstrate the tracking performance. The target is generated according to the system model (eqns. 1–3) and is measured every 0·1 s. The coefficient matrices ϕ, G, H and the computation of Q are the same as in Reference 6 with the coefficient $\alpha = 1/20$ (s^{-1}). The target is in nonmanoeuvring state initially. Within the time interval $k = [400, 700]$, a white process w_k corresponding to a manoeuvre standard deviation $\sigma_m = 100$ (ft/s^2) appears. At time instant $k = 700$, w_k disappears and the acceleration is decremented toward zero gradually. The system returns to a nonmanoeuvring state at time instant $k = 900$ and stays in that state to the end.

This target is tracked by the (modified) manoeuvre detection method with and without the decorrelation process,

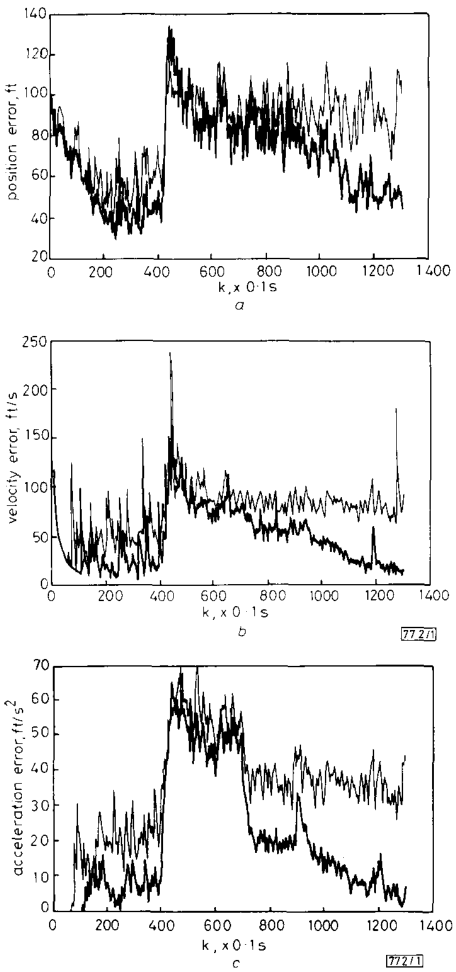

Fig. 1 *Performance (RMS error) of decorrelated and undecorrelated systems in the manoeuvring detection method*

- - - - undecorrelated
——— decorrelated
a Position error
b Velocity error
c Acceleration error

respectively. The parameters $p = 0{\cdot}967$, $t_1 = 60$, $p_2 = 50$, $t_2 = 15$ are used in the simulation. The manoeuvre parameter $\bar{\sigma}_m$ is preset to 100 (ft/s^2) when the system works in manoeuvring mode. Figs. 1*a–c* show the results obtained from this simulation. Initially, both the decorrelated and undecorrelated systems work well in the nonmanoeuvring mode. The decorrelated system has better performance than the undecorrelated system.

When the target is manouevring, both the decorrelated and undecorrelated systems can detect the manoeuvre well and the systems are switched to the manoeuvring mode. A large peak error appears in the short transient period and the decorrelated system may have worse performance than the undecorrelated system in the transient period. Until the steady state is reached, the decorrelation process gives a certain improvement in the error performance.

Up to time instant $k = 700$, the source of manoeuvre variation disappears but the acceleration still exists. The decorrelated system has significantly better performance, particularly in acceleration and velocity estimations, than the undecorrelated system. After time instant $k = 900$, the target reverts to the nonmanoeuvring state. The decorrelation system can detect the nonmanoeuvring state quickly but the undecorrelated system finds it difficult to accomplish the detection. Thus a large error will exist in the undecorrelated system, whereas tremendous improvements in acceleration, velocity, and position performances will be provided by the decorrelation process.

Conclusion: Correlation phenomena in the measurement noise cannot be ignored if the measurement frequency is high enough in many modern radar systems. A modified manoeuvre detection method with the decorrelation process is employed for tracking the manoeuvring target. As shown in Reference 5, this approach has an advantage that the unknown parameters about noise correlation can be easily estimated. From computer simulation, it can be seen that the system performance can be improved significantly if the effect of noise correlation is considered. The situation where the target reverts from the manoeuvring to nonmanoeuvring state is difficult to detect in the undecorrelated system, whereas it is no problem to make this detection in the decorrelated system.

J.-A. GUU
C.-H. WEI

Institute of Electronics
National Chiao Tung University
Hsin Chu, Taiwan, Republic of China

13th December 1990

References

1 CHANG, C. B., and TABACZYNSKI, J. A.: 'Application of state estimation to target tracking', *IEEE Trans.*, 1984, **AC-29**, pp. 98–109
2 ROGERS, S. R.: 'Alpha–beta filter with correlated measurement noise', *IEEE Trans.*, 1987, **AES-23**, pp. 592–594
3 GUU, J. A., and WEI, C. H.: 'A maneuvering target tracking system with correlated measurement noises'. IEEE 1990 Intern. Radar Conf., Arlington, VA, USA, pp. 451–455
4 GUU, J. A., and WEI, C. H.: 'Maneuvering target tracking using IMM method at high measurement frequency', to be published in *IEEE Trans.*, 1991, **AES-27**
5 GUU, J. A., and WEI, C. H.: 'Simple parameter estimation technique in manoeuvring target tracking system', *Electron. Lett.*, 1990, **26**, pp. 508–509
6 SINGER, R. A.: 'Estimating optimal tracking filter performance for manned maneuvering targets', *IEEE Trans.*, 1970, **AES-6**, pp. 473–483
7 BAR-SHALOM, Y., and BIRMIWAL, K.: 'Variable dimension filter for maneuvering target tracking', *IEEE Trans.*, 1982, **AES-18**, pp. 621–629

HIGH PERFORMANCE HYBRID CIRCUIT MODULES FOR LIGHTWAVE SYSTEMS OPERATING AT DATA RATES OF 10 Gbit/s AND HIGHER

Indexing terms: Hybrid integrated circuits, Multiplexers, Bipolar devices, Optical communication

Two hybrid circuit modules, an 11 Gbit/s 1 : 2 demultiplexer and a 12 Gbit/s 2 : 1 multiplexer, are described. The modules use silicon bipolar integrated circuits and feature multiple input/output connectors, excellent insertion and return losses, and flat group delays.

Introduction: Recently, there has been considerable interest in integrated circuits (ICs) and IC technologies for lightwave communication systems operating at next generation SONET rates of 10 Gbit/s and beyond.[1–3] For example, multiplexer ICs have been reported for gallium arsenide heterojunction bipolar transistors (HBTs),[4] high electron mobility transistors,[5] and silicon bipolar technologies, operating at 15, 12, and 11·4 Gbit/s, respectively. Generally, wafer probes have been used to characterise these advanced ICs. However, wafer probing is impractical for prototyping systems requiring multiple ICs. In addition, wafer probe characterisation does not address practical system considerations such as the need for electromagnetic interference (EMI) shielding, the inability to couple light effectively into optoelectronic ICs (OEICs), restrictions in the number and characteristic impedance of signal lines, and the difficulties encountered when interconnecting ICs on a single substrate. These issues can be overcome with hybrid ICs (HICs).

We describe two hybrid circuit modules, a high input sensitivity 11 Gbit/s 1 : 2 demultiplexer and a 12 Gbit/s 2 : 1 multiplexer, which overcomes these limitations. The modules use previously reported silicon bipolar ICs,[6,7] mounted inside a high performance coplanar universal mount test fixture. Both circuit modules achieve comparable or superior performance to previous wafer-probed results. The performance of the coplanar fixture is characterised up to 30 GHz.

Coplanar fixture design: The coplanar fixture is a universal 2·5 cm × 5 cm × 1 cm structure that allows for a maximum of 12 input/output signal lines, with an additional four power supply connections (Fig. 1). Mounted inside the fixture is a

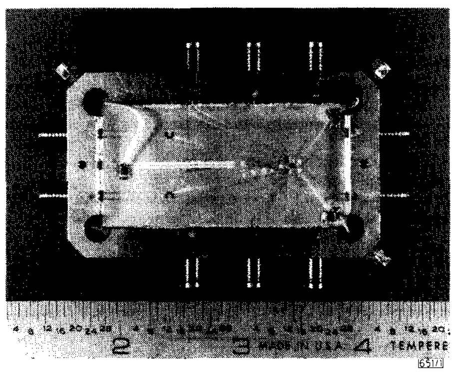

Fig. 1 *Photograph of coplanar universal mount test fixture*

0·64 mm thick ceramic ($\varepsilon_r = 9{\cdot}9$) substrate with coplanar waveguides etched on the 5 μm gold plated top surface (there is no metallisation on the lower surface). Thin-film resistors are etched on a 50 Ω/□ TaN layer. Around the circumference of the fixture, Wiltron K connectors on a 1·25 cm centre-to-centre pitch launch onto the substrate. The substrate is soldered or conductive epoxied to the walls of the fixture, creating a uniform and low inductance ground. Periodically bridged over the coplanar waveguides' centre conductor, wire bonds aid in suppressing moding between sections of the ground. Bypass chip capacitors are epoxied to ground as close as possible to the power supply bond pads of the ICs to suppress undesirable noise. Larger surface-mount ceramic capacitors, mounted on internal power supply lines, also aid noise suppression.